Proceedings of the American Control Conference
San Diego, California • June 1999

ACCELERATION FEEDBACK DESIGN FOR VOICE COIL ACTUATED DIRECT DRIVE*

Alex Babinski
ababinsk@uiuc.edu
Tsu-Chin Tsao
t-tsao@uiuc.edu
Department of Mechanical and Industrial Engineering
University of Illinois at Urbana-Champaign
Urbana, Illinois

Abstract

Development of a servo-control system for a voice coil actuated direct drive used in turning of automotive camshafts is presented. The drive must possess low inertia, in order to satisfy motion bandwidth requirements for cam turning with a small actuator. Reduced inertia, however, makes the system more sensitive to the external forces acting on the drive, and may lead to chatter during cutting. High dynamic stiffness must be established by the control system to minimize the effects of the additional dynamics introduced by the machining process. This work presents a systematic approach to design of local acceleration feedback to increase the dynamic stiffness of the drive. An acceleration loop is added to the drive's servo-controller, that consists of an aggressive position feedback and a feedforward controller, resulting in a five-fold improvement in the system's performance.

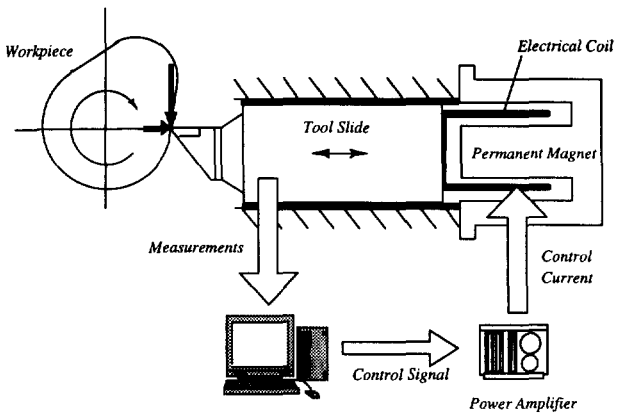

Fig. 1: System Setup. Voice Coil Actuated Drive Used for Turning of Camshafts.

1 Introduction

In recent years direct drive machining attracted significant amount of attention because of the advantages of this technology over conventional machining techniques. Linear actuators, such as voice coils, can be used in low inertia, high precision servo-systems that are capable of motion with very high velocity and acceleration. High achievable motion bandwidth makes these drives ideal for high-speed machining applications such as noncircular turning (Fig.1), where the conventional drives are not suitable. The absence of the transmission mechanism is the main advantage of direct drives. However, it is also the source of concerns for process stability. Voice coils, similar to other types of electric motors, have zero stiffness; and because of the light weight and absence of the gear reduction mechanism or a lead screw, the system is sensitive to the forces that arise from the interaction of the drive with the machining process. A proper system stiffness must be established by the control system to ensure stable and low vibration machining operation.

Cutting process stability in connection with direct drive machining was considered by Alter and Tsao [1994]. An additional feedback loop exists in the system during machining, since the cutting force is a function of the tool position. As suggested by the small gain theorem, in order to guarantee stability, it is necessary to minimize drive gain. Namely, let T_{xw} and Δ_c denote the system's compliance[1] and cutting process respectively. Suppose that the cutting process is l_2-stable, and let $\|\Delta_c\|_\infty < \gamma$. Then, the stability will be guaranteed if

$$\|T_{xw}\|_\infty < \frac{1}{\gamma}. \tag{1}$$

Since the process gain γ is a function of cutting conditions, the control system design objective is to minimize $\|T_{xw}\|_\infty$ to improve system robustness for general purpose machining. The problem is posed in an optimal control framework and an aggressive position feedback can be designed using $\mathcal{H}_\infty$ method as a tool for obtaining a controller (Alter and Tsao [1996]). To minimize errors due to a large DC component of the cutting force, weighting filters in an $\mathcal{H}_\infty$ problem setup must have large magnitude at low frequencies to yield a controller with a pole close to the origin. The aggressiveness of the control system (i.e. the achievable dynamic stiffness) is limited by the considerations of robustness with respect to uncertain high frequency drive dynamics, as described in Section 2.

Improvement of disturbance rejection characteristics of electric drives was addressed by many researchers. Ohnishi [1987] and Umeno and Hori [1991] introduced a disturbance observer to handle the external disturbances. In this approach, an equivalent disturbance was estimated using an inverse model of the plant; this estimate was then used to calculate an additional control signal to cancel the disturbance. Schmidt and Lorenz [1992] considered the use of acceleration feedback in control of DC drives. It was shown that acceleration feedback acts as an "active inertia" and can be used to produce higher stiffness. In this work an observer to estimate an acceleration signal using velocity measurements was utilized. $\mathcal{H}_\infty$ optimal force feedback was considered by Alter and Tsao [1994]. Actual online measurement from a force dynamometer was added to the position control system to increase the stiffness of the drive by approximately 100%.

This paper presents a systematic approach to design of local acceleration feedback to improve the system performance beyond the level achievable with the position feedback alone. Limitations of the position based control, the need in additional sensor feed-

*This work was supported in part by NIST Advanced Technology Program.

[1]Compliance is the mapping from disturbance to position, i.e. it is a scalar inverse of stiffness.

back, and implementation of acceleration feedback are discussed in Section 2. It is shown that any stabilizing controller can be represented in a form where acceleration feedback is realized as a local internal model controller, which presents a number of practical advantages. The derived robust stability condition illustrates the benefits of the additional sensor feedback. The description of the voice coil drive and experimental results are presented in Section 3, followed by conclusions in Section 4.

2 Design of the Acceleration Feedback

An idealized model of the system dynamics for the tool slide driven by a voice coil is given by

$$m\ddot{x} + c\dot{x} = k_i k_u u + w, \tag{2}$$

where x is the displacement of the tool, m is the mass of the moving portion of the drive, c is the equivalent viscous damping, k_i and k_u are the proportionality constants between the control input to the power amplifier, u, and the force generated by the motor, $F_c = k_i k_u u$, and w is the disturbance (cutting) force acting on the tool.

Using position as a feedback signal a controller to stabilize the system and meet certain performance specifications can be designed. A typical position feedback compliance curve is shown in Fig.5 as a dashed line. Reducing the peak of the compliance at higher frequencies is a challenging task. Since the disturbance force is at the plant input a controller has access to information that is filtered by the system. As can be seen from the Bode plot of the system (2), the high frequency components of the disturbances contained in the position signal are attenuated and delayed by the plant. Therefore, a position based control system requires high controller gains and precise knowledge of the real system to "catch up" with the disturbances. But, since the model at high frequencies is usually uncertain[2] the high controller gain may result in instability. This suggests that additional process information may be required in order to fully utilize the potential of the system.

It is well known that excellent stability margins and superior performance of state feedback schemes are difficult to recover in observer based designs, because of fundamental limitations of output feedback. Observers use output signal for state (or other variable) reconstruction and require good system model to maintain stability. Therefore, to improve the system performance, a fast sensor such as an accelerometer or a force dynomometer has to be used for feedback. Using force measurements is not practical for many applications, because a force dynomometer will increase the inertia of the system, have compliance itself, and is not as cost effective as using an accelerometer. The motivation for using acceleration feedback to reject dynamic loads acting on the drive is quite clear. As can be seen from equation (2), an acceleration signal contains direct unfiltered information about the exogenous force, w, and the control system will react faster to cancel the disturbance.

A special controller structure for a system with position and acceleration measurements is proposed in Fig.2. Practical advantages of using local internal model controller[3] for acceleration feedback become apparent by inspecting the transfer function for the controlled variable:

$$x = \frac{KG_x}{1+KG_x} G_{ff} r_d + (1 - HG_a)\frac{G_x}{1+KG_x} w. \tag{3}$$

In this configuration the system's disturbance rejection characteristics can be addressed directly by the acceleration feedback, while the reference-to-position mapping of the position based system remains unaffected. This means that a plug-in acceleration module can be added to the existing controller to shape the system compliance, T_{xw}, when necessary. The task of reducing the $\mathcal{H}_\infty$ norm of compliance is accomplished by minimizing $\|W_a(1 - HG_a)\|_\infty$, where W_a specifies the desired frequency range (say where it is). Low tracking controller order is yet another advantage of this structure, since tracking schemes involve inversion of T_{xr} that is not affected by the additional sensor loop. The system remains stable if acceleration loop is turned off, and its plug-in form offers the convenience of tuning the system in a loop-by-loop fashion. Notice that the control system contains the model of the acceleration output. However, it is not used for reconstruction of signals; rather it appears in the additional sensor loop as part of internal model control structure - a parameterization of all stabilizing controllers for stable plants.

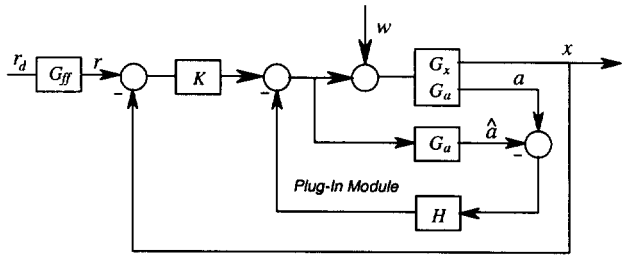

Fig. 2: Addition of a Local Acceleration Feedback Loop to the System.

Lemma 1 *For a 2×1 plant $G = [G_1\ G_2]^T$ with $G_2 \in \mathcal{RH}_\infty$, all stabilizing controllers are given by*

$$u = v_0^{-1} q_2 (y_2 - G_2 u) + v_0^{-1} \left(u_0 y_1 + q_1 (m y_1 - n u)\right), \tag{4}$$

where u is the control signal, y_1 and y_2 are measurements, $m, n, u_0, v_0, q_1, q_2 \in \mathcal{RH}_\infty$, and

$$G_1 = nm^{-1}, \tag{5}$$

$$v_0 m - u_0 n = 1. \tag{6}$$

Proof. Noting that $G_2 \in \mathcal{RH}_\infty$, the plant is stabilized by a controller $K_0 = u_0/v_0$, where stable transfer functions u_0 and v_0 satisfy the Bezout identity $v_0 m - u_0 n = 1$.

Let

$$G = \begin{bmatrix} G_1 \\ G_2 \end{bmatrix} = NM^{-1} = \begin{bmatrix} n \\ n_2 \end{bmatrix} m^{-1} \tag{7}$$

be the right coprime, and

$$G = \begin{bmatrix} G_1 \\ G_2 \end{bmatrix} = \tilde{M}^{-1}\tilde{N} = \begin{bmatrix} m & 0 \\ 0 & 1 \end{bmatrix}^{-1} \begin{bmatrix} n \\ G_2 \end{bmatrix} \tag{8}$$

the left coprime factorization of G over $\mathcal{RH}_\infty$. Then all stabilizing controllers are given by

$$C = \left(\tilde{V}_0 + Q\tilde{N}\right)^{-1} \left(\tilde{U}_0 + Q\tilde{M}\right), \tag{9}$$

where $\tilde{U}_0$, $\tilde{V}_0 \in \mathcal{RH}_\infty$ satisfy the Bezout identity

$$\tilde{V}_0 M - \tilde{U}_0 N = 1. \tag{10}$$

[2] At high frequencies the system (input-to-position) behaves approximately as a double integrator and is difficult to identify due to the low amplitude of the position signal.

[3] In internal model control, the difference between the measured and simulated outputs, which reflects the disturbance acting on the plant, is passed through a controller, H, to generate control signal to compensate the disturbance.

It is straightforward to verify that the choice

$$\tilde{V}_0 = v_0, \quad \tilde{U}_0 = [u_0\ 0] \tag{11}$$

satisfies the above identity. Noting (8) and (11) all stabilizing controllers (9) are shown in Fig.3 and (4) follows directly. Q.E.D.

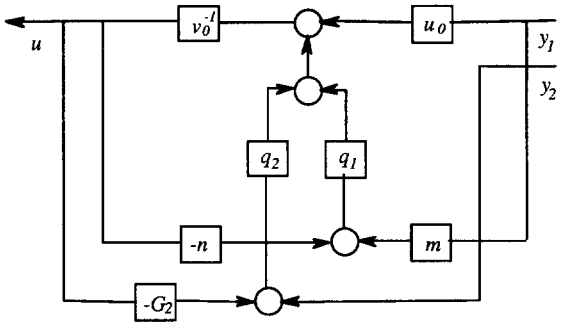

Fig. 3: Youla Parameterization of All Stabilizing Controllers.

It is established next that (4) and the structure in Fig.2 are equivalent.

Theorem 2 *All stabilizing controllers are given by*

$$u = -Ky_1 - H(y_2 - G_2 u), \tag{12}$$

where

$$K = -\frac{u_0 + q_1 m}{v_0 + q_1 n}, \tag{13}$$

through a parameterization

$$H = -\frac{q_2}{(v_0 + q_1 n)}. \tag{14}$$

The result follows by substituting (14) into (4). Note that, unlike the regular model reference controller, H can be unstable if $(v_0 + q_1 n)$ is not invertible in $\mathcal{RH}_\infty$, and the unstable zeros are not cancelled by q_2. Rewriting (14) as $q_2 = -(v_0 + q_1 n)H$, it can be seen that if the second sensor loop is designed as an addition to the position based system, and $H \in \mathcal{RH}_\infty$, the closed loop system will be stable.

Next, a robust stability condition is derived for the model set characterized by multiplicative perturbations of the nominal model $G = [G_x\ G_a]^T$. Since the system has one input, and in the swept sine experiment (that is used for system identification in Section 3) actuator and sensor uncertainties are indistinguishable, both types of uncertainty are absorbed into the output uncertainty as shown in Fig.4. For brevity, the closed-loop system is referred to as $\mathcal{F}[\cdot, (\cdot, \cdot)]$.

Theorem 3 *Let the plant, $\tilde{G} = [\tilde{G}_x\ \tilde{G}_a]^T$, belong to the set Γ,*

$$\Gamma = (I + \hat{\Delta}W)G, \quad \hat{\Delta} = \begin{bmatrix} \hat{\Delta}_1 & 0 \\ 0 & \hat{\Delta}_1 \end{bmatrix}, \quad W = \begin{bmatrix} W_1 & 0 \\ 0 & W_2 \end{bmatrix}, \tag{15}$$

where G is the system model, $\hat{\Delta}_i$, $W_i \in \mathcal{RH}_\infty$, $\|\hat{\Delta}_i\|_\infty \leq 1$. Suppose that $\mathcal{F}[G, (K, H)] \in \mathcal{RH}_\infty$. Then, $\mathcal{F}[\Gamma, (K, H)] \in \mathcal{RH}_\infty$ ($\mathcal{F}[\tilde{G}, (K, H)] \in \mathcal{RH}_\infty$) iff (if)

$$\left| W_1 \frac{KG_x}{1 + KG_x} \right| + \left| W_2 \frac{HG_a}{1 + KG_x} \right| < 1, \quad \omega \in \mathbb{R}_+. \tag{16}$$

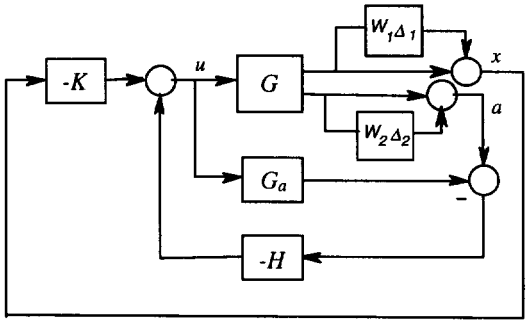

Fig. 4: Robust Stability Analysis of the System with Uncertainty Represented as a Multiplicative Output Perturbation.

Proof. The system shown in Fig.4 is robustly stable iff (Doyle *et al.* [1982])

$$\sup_{\omega \in \mathbb{R}_+} \mu_{\mathbf{\Delta}}(M(j\omega)) < 1, \tag{17}$$

where

$$\mathbf{\Delta} = \{diag[\Delta_1, \Delta_2] : \Delta_i \in \mathbb{C}\}, \tag{18}$$

$$M = \begin{bmatrix} -W_1 \dfrac{KG_x}{1 + KG_x} & -W_1 \dfrac{HG_x}{1 + KG_x} \\ -W_2 \dfrac{KG_a}{1 + KG_x} & -W_2 \dfrac{HG_a}{1 + KG_x} \end{bmatrix}. \tag{19}$$

For each frequency ω, $\mu_{\mathbf{\Delta}}$ is calculated as

$$\mu_{\mathbf{\Delta}}(M(j\omega)) = \inf_{d_\omega \in \mathbb{R}_+} \bar{\sigma}(D_\omega^{-1} M D_\omega), \quad D_\omega = diag[d_\omega, 1]. \tag{20}$$

It is straightforward to show that

$$\bar{\sigma}(D_\omega^{-1} M D_\omega) = \frac{(|W_1 G_x|^2 + d_\omega^2 |W_2 G_a|^2)(|H|^2 + d_\omega^2 |K|^2)}{d_\omega^2 |1 + KG_x|^2}, \tag{21}$$

and is minimized by

$$d_\omega^* = \sqrt{\left| \frac{W_1 HG_x}{W_2 KG_a} \right|} \tag{22}$$

yielding

$$\mu_{\mathbf{\Delta}}(M(j\omega)) = \left| W_1 \frac{KG_x}{1 + KG_x} \right| + \left| W_2 \frac{HG_a}{1 + KG_x} \right|. \quad \text{Q.E.D.} \tag{23}$$

Condition (16) (which can be written as $|W_1 T| + |W_2 HG_a S| < 1$, where S and T are position feedback sensitivity and complementary sensitivity functions respectively) can be used for robust stability analysis of the additional feedback loop. Uncertainty of the system model imposes limitations on system bandwidth because the position controller has to roll-off at higher frequencies to satisfy the robust stability condition $|W_1 T| < 1$. The peak of the compliance takes place around the cross-over frequency where both $|W_1 T|$ and $|S|$ approach unity. For the acceleration feedback to be effective it is necessary that $|HG_a| \approx 1$; therefore, it follows from (16) that in order to reduce the compliance, $|W_2| \ll 1$ must be satisfied in the desired frequency range. This illustrates the benefits of using an additional sensor over the "deriving" the desired signal from another signal that is already used for feedback. For example, using differentiation of position to obtain acceleration for control amounts to setting $W_2 = s^2 W_1$, and may lead to stability problems in a real system.

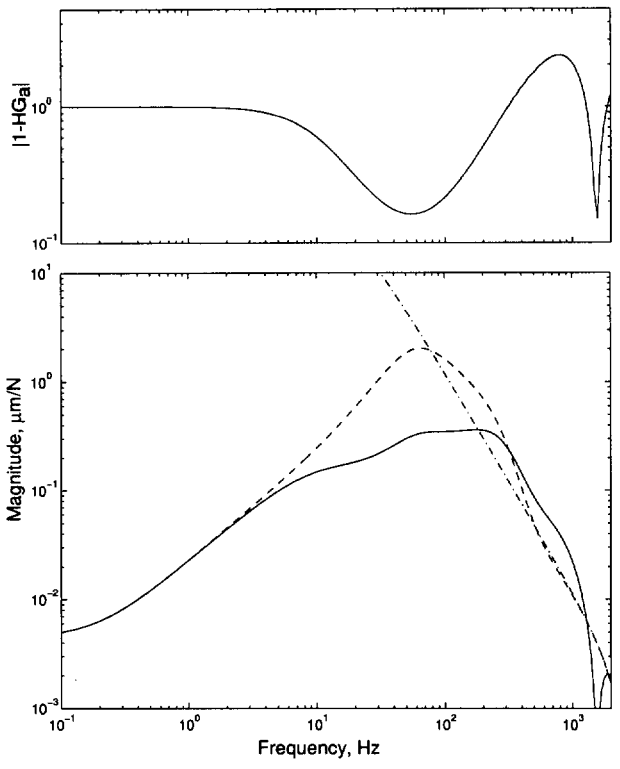

Fig. 5: System Compliance. Top - Magnitude of the "Acceleration Loop," Bottom - Compliance With (solid) and Without (dashed) Acceleration Feedback, and the Plant (dash-dot).

3 Experimental Results

The experimental system consists of a linear tool slide (moving mass $1.5kg$) driven by a voice coil actuator (mass of the coil $0.6kg$). The $10sec$ peak and continuous stall force of the actuator are $1670N$ and $320N$ respectively. The actuator is powered by a PWM servo-amplifier. Static force sensitivity between the input to the amplifier and the force generated by the voice coil was set at $115N/V$. A laser Doppler sensor with 0.628 μm resolution is used for measuring the position of the tool. A piezoelectric accelerometer with sensitivity $\rho = 95.0mV/g = 0.0097Vsec^2/m$ is used to measure the acceleration. A first order filter with cut-off at $500Hz$ was used to attenuate high frequency acceleration noise generated by the switching in the power amplifier. The control algorithm was implemented on TMS320C32 floating point digital signal processor.

Frequency response of the slide (from the input to the amplifier to the position measured by the laser sensor) is shown in Fig.6 as solid lines for various level of the excitation signal. Sampling frequency of $5000Hz$, and the following discrete model

$$G_x(z^{-1}) = 10^{-3}\frac{z^{-3}(1.06 + 1.05z^{-1})}{1 - 1.97z^{-1} + 0.97z^{-2}},\ [mm/V] \qquad (24)$$

shown in Fig.6 as a dashed line, was used for position feedback design. This model is a zero-order-hold equivalent of the continuous model (2) delayed by two sampling intervals, which were used to approximate the power amplifier dynamics in the frequency range of interest (below $1kHz$). The mismatch of the model and experimental curves in the low frequency range is due to the Coulomb friction. An aggressive feedback controller, K, was designed using MATLAB μ-Tools package from MathWorks Inc. To reduce tracking errors a noncausal feedforward controller (Tsao [1994]) was added to the system. The compliance transfer function for the system is shown in Fig.5 as a dashed line.

Frequency responses from input to the amplifier to the filtered output of the accelerometer signal conditioner are shown in Fig.7 as solid lines. Dashed line corresponds to the model,

$$G_a(z^{-1}) = \frac{z^{-3}(0.24 - 0.24z^{-1})}{1 - 1.50z^{-1} + 0.52z^{-2}}\ [V/V]. \qquad (25)$$

This model is a delayed by two sampling intervals zero-order-hold equivalent of (2) filtered by a first order filter.

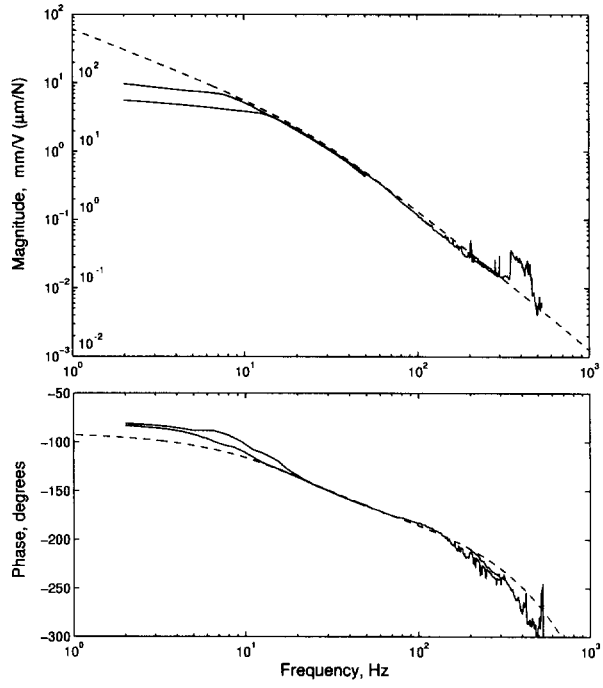

Fig. 6: Open Loop Frequency Response (position). Experimental Data for Various Level of Excitation (solid) and the System Model (dashed).

Since the μ-Tools package is suited for design of feedback controllers, the model matching problem was converted to a conventional weighted sensitivity minimization problem in terms of a controller, N, using a parameterization $H = N/(1+NG_a)$. The error was heavily weighted in the mid-frequencies where the compliance reaches its maximum. Weighting filters on noise and control had large magnitude in the very low and very high frequency ranges. The magnitude of the "acceleration loop," $|1 - HG_a|$, and the resulting system compliance curve are shown in Fig.5. It can be seen that $\|\hat{T}_{xw}\|_\infty$ is reduced from $2.03\mu m/N$ to $0.36\mu m/N$, i.e. the stiffness of the system is increased by 563%. Comparison of the theoretical compliance with the results of an impact hammer test is shown in Fig.8. Figure 9 presents the results of the experiment where an impact disturbance was simulated by adding to the control signal a $1V$ ($115N$) burst for the duration of $4msec$. The error of the system with the acceleration loop is shown as the solid line, and the dashed line corresponds to the case when the acceleration loop is turned off.

Tracking error for the trajectory corresponding to an automotive cam used in production (for spindle speed of $600rpm$ maximum tool travel, velocity, and acceleration are $6.5mm$, $0.6m/sec$, and $98.2m/sec^2$ respectively) is presented in Fig.10. Reduction of the tracking error with addition of the acceleration loop can be explained as follows. The tracking error in this experiment (conducted without cutting) is primarily due to the dynamics that are not captured by T_{xr} used for the feedforward controller design. In certain sense, unmodeled dynamics can be viewed as disturbance,

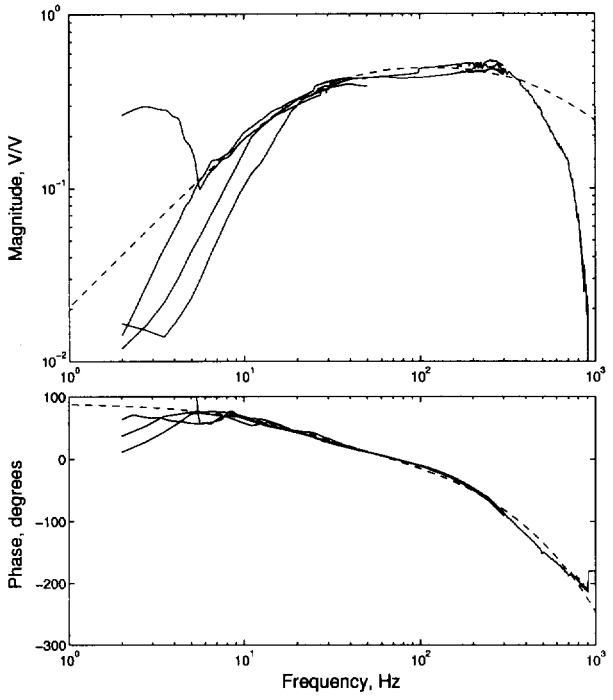

Fig. 7: Open Loop Frequency Response (acceleration).

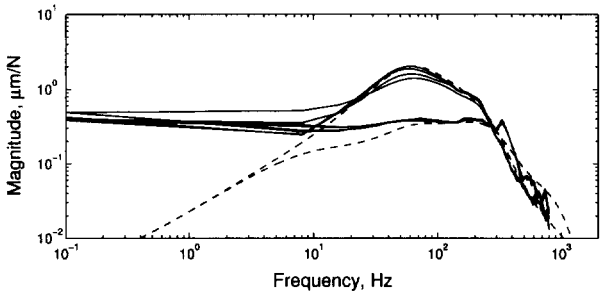

Fig. 8: Impact Hammer Test. Comparison of Theoretical (dashed) and Experimental (solid) System Compliance.

which will be attenuated by the acceleration feedback. FFT analysis of the error signal reveals that there are large magnitude components at frequencies around $50Hz$, which belongs to the range where acceleration feedback provides the most improvement.

4 Conclusion

To guarantee stability, direct drive machining systems must possess adequate stiffness characteristics. The information about disturbances contained in the position signal is delayed and attenuated by the plant. To provide high stiffness in higher frequency range additional information from a fast sensor that reflects the disturbances without delay is necessary. It was demonstrated that by adding the acceleration feedback loop to the position based system, the system stiffness could be increased by approximately 5.6 times.

References

[1] Alter, D.M., and Tsao, T.-C., 1994, "Stability of Turning Processes with Actively Controlled Linear Motor Feed Drives," *ASME J. Dyn. Sys., Meas., and Contr.*, Vol. 116, pp. 298-307.

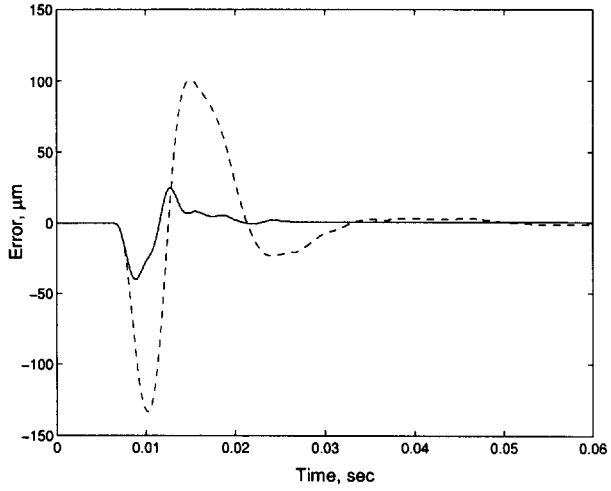

Fig. 9: Time Response to an Impact Disturbance With (solid) and Without (dashed) Acceleration Feedback.

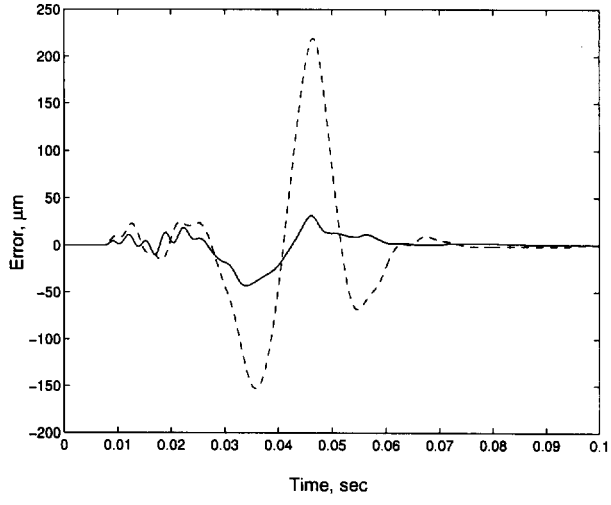

Fig. 10: Tracking Error Using the Same Feedforward Controller; With (solid) and Without (dashed) Acceleration Feedback.

[2] Alter, D.M., and Tsao, T.-C., 1996, "Control of Linear Motors for Machine Tool Feed Drives: Design and Implementation of $\mathcal{H}_\infty$ Optimal Feedback Control," *ASME J. Dyn. Sys., Meas., and Contr.*, Vol. 118, pp. 649-656.

[3] Doyle, J.C., Wall, J.E., and Stein, G., 1982, "Performance and Robustness Analysis for Structured Uncertainty," *Proc. IEEE Conf. Dec. and Contr.*, pp. 629-636.

[4] Ohnishi, K., 1987, "A New Servo Method in Mechatronics," *Trans. Jap. Soc. El. Eng.*, Vol. 107-D, pp. 83-86.

[5] Schmidt, P.B., and Lorenz, R.D., 1992, "Design Principles and Implementation of Acceleration Feedback to Improve Performance of DC Drives," *IEEE Trans. Indust. Appl.*, Vol. 28, No.3, pp. 594-599.

[6] Tsao, T.-C., 1994, "Optimal Feed-Forward Digital Tracking Controller Design," *ASME J. Dyn. Sys., Meas., and Contr.*, Vol. 116, pp. 583-592.

[7] Umeno, T., and Hori, Y., 1991, "Robust Speed Control of DC Servomotors Using Modern Two-Degrees-of-Freedom Controller Design," *IEEE Trans. on Indust. Electronics*, Vol. 38, No.5, pp. 363-368.